Effect of hydrogen dilution on the structure of SiOF films prepared by remote plasma enhanced chemical vapor deposition from SiF_4-based plasmas

J. C. Alonso,[a] E. Pichardo, V. Pankov, and A. Ortiz
Instituto de Investigaciones en Materiales, Universidad Nacional Autónoma de México, AP 70-360, 04510 México D. F., México

(Received 13 October 1999; accepted 17 July 2000)

Structural and electrical properties of fluorinated silicon dioxide (SiOF) films prepared by remote plasma enhanced chemical vapor deposition from the SiF_4–O_2–H_2–He gas mixture have been studied using ellipsometry, Fourier transform infrared spectroscopy, transmission electron microscopy, and current–voltage measurements. It has been found that the level of hydrogen dilution strongly affects the microstructure of deposited SiOF films. The films prepared at the H_2 flow rate below about 0.8 sccm have a biphase structure consisting of an amorphous matrix with the incorporation of 5–30 nm sized particles. The main origin of these particles seems to be gas phase oxidation of SiF_x species (with $x=1$, 2, 3) in plasma and downstream regions. Resulting films are characterized by extremely low density, reduced structural homogeneity, and poor electrical properties. Increase in the H_2 flow rate above 0.8 sccm completely suppresses the incorporation of particles into the growing film probably due to effective hindering gas phase oxidation process and results in dense homogeneous amorphous SiOF films with good electrical properties. © *2000 American Vacuum Society.* [S0734-2101(00)01506-8]

I. INTRODUCTION

The main trend of the modern ultralarge scale integration circuits industry towards device shrinking has aroused a great deal of interest in low dielectric constant materials whose application as an interlayer insulator enables strong reduction in wiring capacitance of multilevel metallization. Among these materials, fluorinated SiO_2 (SiOF) is one of the best candidates because of its easy integration into existing semiconductor processing along with excellent insulating,[1,2] gap filling properties,[3,4] and dielectric constant as low as 3.6.[2]

SiH_4,[5] Si_2H_6,[1] tetra-ethoxy-silane,[3,6–11] and other organosilanes have been used recently as a silicon source for plasma enhanced chemical vapor deposition (PECVD) of SiOF films. However SiOF films obtained from these precursors usually contain hydrogen bonded in Si–H and Si–OH groups,[7,9,12] which causes moisture instability problems during the postdeposition period. To avoid hydrogen incorporation into the SiOF film, hydrogen-free SiF_4-based plasmas have been applied recently in several studies.[6,13–16] However, the question about the optimal feedstock gas mixture still remains open.

In our previous study it was shown that hydrogen addition to SiF_4-based plasmas enables one to control the fluorine doping level of SiOF films without hydrogen incorporation into the film.[17] However, other reasons exist for hydrogen addition to SiF_4-based plasmas. It has been revealed recently that hydrogen dilution can cause considerable improvement in the structure of μc-Si:H films prepared by PECVD from SiH_4–H_2 plasma.[18] The results of our previous studies[19] allow us to suppose that an increasing amount of H_2 in the reaction chamber causes densification of silicon dioxide films prepared by direct PECVD from SiF_4–NO_2–H_2 gas mixture. The purpose of this work is to study in detail the effect of hydrogen addition to the process on the microstructure of SiOF films prepared by remote PECVD from SiF_4-based plasmas using laser ellipsometry, Fourier transform infrared (FTIR) spectroscopy, and transmission electron microscopy characterization techniques. Since the main application of SiOF films is to serve as an interlayer dielectric of the integrated circuits with multilevel metallization, it is of practical interest to study the correlation between the structural changes observed in SiOF films as a function of H_2 flow rate and the electrical properties of these films.

II. EXPERIMENT

SiOF films were prepared by the remote PECVD technique using SiF_4–O_2–H_2–He feedstock gas mixtures. The reaction chamber was equipped by an inductively coupled plasma source mounted on the top flange. The detailed geometry of the reaction chamber is described elsewhere.[17] The films were deposited on n-type (100) silicon substrates of 200 Ω cm. To study the effect of hydrogen dilution on the deposition of SiOF films, SiF_4, O_2, and He flow rates were kept constant at 20, 40, and 280 sccm while the hydrogen flow rate was varied from 0 to 10 sccm. For special studies a SiF_4 flow rate of 5 sccm was applied. The total pressure was held at 500 mTorr using a throttle valve for all deposition cycles. The substrate temperature during film deposition was 175 °C. The plasma was generated and sustained by applying 200 W of a 13.56 MHz radio frequency power for all depositions.

[a]Electronic mail: alonso@servidor.unam.mx

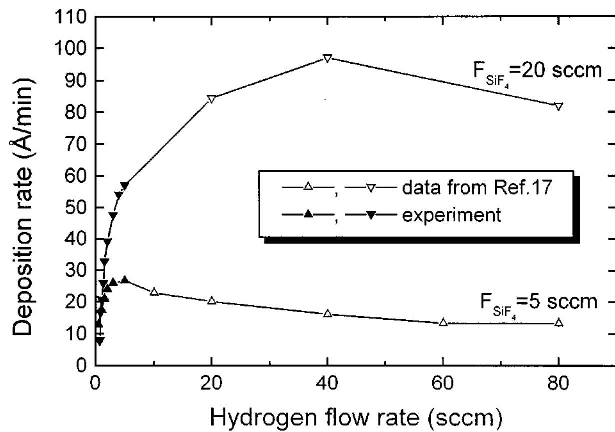

FIG. 1. Deposition rate of SiOF films vs H_2 flow rate at different values of SiF_4 flow rate.

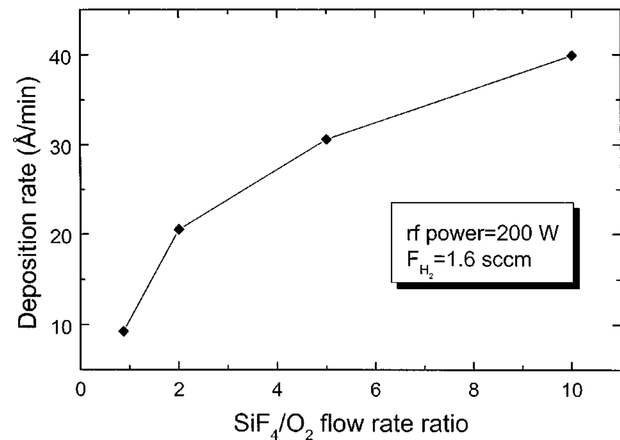

FIG. 2. Deposition rate of SiOF films vs SiF_4/O_2 flow rate ratio.

Film thickness and refractive index were measured using a Gaertner L117 laser ellipsometer. Films thickness was targeted for 1000 Å. Film composition and structure was studied by FTIR absorption spectrometer Nicolet 210. The ratio of the area of 900–1000 cm^{-1} Si–F_x absorption band to the area of the stretching mode Si–O peak (Si–F/Si–O ratio) was used after base line correction for qualitative estimation of fluorine content in the SiOF films. IR measurements were used to study the microstructure of our films as a function of fluorine content. For this purpose we used a procedure based on the central force model of Sen and Thorpe,[20] which was developed in the past to study the structure of thermal and device quality SiO_2 films[21,22] and has been applied recently to study SiOF films.[13] This procedure consists in using the relation between the peak position and change in full width at half maximum (FWHM) of the main Si–O–Si phonon band within the SiOF network and the width of Si–O–Si bond angle distribution (Si–O–Si angle deviation), which is a direct indicator of film microstructure. On the other hand, based on several articles related to the topic,[23–33] the ratio between the IR absorption intensity of the high-wave number shoulder and the main peak of the Si–O–Si stretching vibration mode in SiO_2 was used to evaluate the structural properties and porosity of our SiOF films. Film microstructure was further examined by electron microscope Jeol-1200EX in bright-field, dark-field, and selected area electron diffraction regimes. Electrical measurements were performed using metal–oxide–semiconductor (MOS) structures fabricated on crystalline n-type silicon wafers of 0.1–1 Ω cm. The metal contacts were aluminum dots with 0.14 cm diam thermally evaporated through a metallic mask. The current–voltage (I–V) characteristics were measured with a log-picoammeter and a ramp voltage generator.

III. RESULTS

A. Deposition rate, fluorine content and structure

Figure 1 shows the film deposition rate as a function of H_2 flow rate for two SiF_4 flow rates, 5 and 20 sccm. No film growth is observed when hydrogen-free SiF_4–O_2–He gas mixture is applied. SiOF film growth starts only when hydrogen is added into the feedstock gas mixture at flow rates higher than 0.6 sccm. For both SiF_4 flow rates, first an increase in the deposition rate is observed (Fig. 1) as the H_2 flow rate increases, then, after reaching a maximum value, which depends on the SiF_4 flow rate, the deposition rate decreases as a function of hydrogen flow rate. The effect of SiF_4/O_2 flow rate ratio on the deposition rate of oxides deposited at low hydrogen flow rate (1.6 sccm) is shown in Fig. 2. It is observed that under these conditions the deposition rate increases as the SiF_4/O_2 ratio increase.

Figure 3 shows the refractive index of SiOF films as a function of H_2 flow rate. As seen in the figure, the refractive index of the films prepared at 0.8–5 sccm of H_2 flow rate is in the 1.398–1.417 range, but drops sharply up to the value of 1.2 when the H_2 flow rate is reduced below 0.8 sccm. In order to study the origin of lower refractive index of our SiOF films, studies of F content and film microstructure were performed.

The incorporation of fluorine in our SiOF films was studied by IR measurements. A typical FTIR spectrum of our samples is shown in Fig. 4. It contains three major peaks located at 1090, 800, and 450 cm^{-1} (see Fig. 4) that are usually identified as the stretching, bending, and rocking

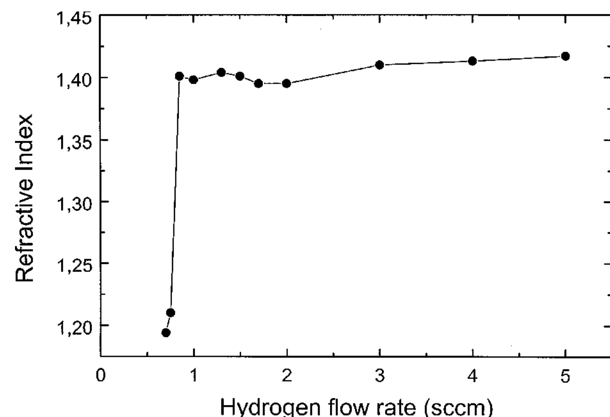

FIG. 3. Refractive index of SiOF films vs H_2 flow rate.

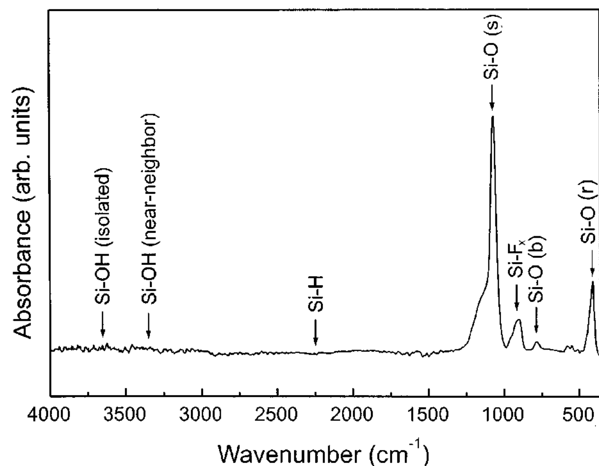

FIG. 4. Typical FTIR spectrum of the SiOF film prepared at H_2 flow rate of 1.5 sccm. Si–O–Si stretching, bending and rocking vibrational modes are labeled as (s), (b), and (r), respectively.

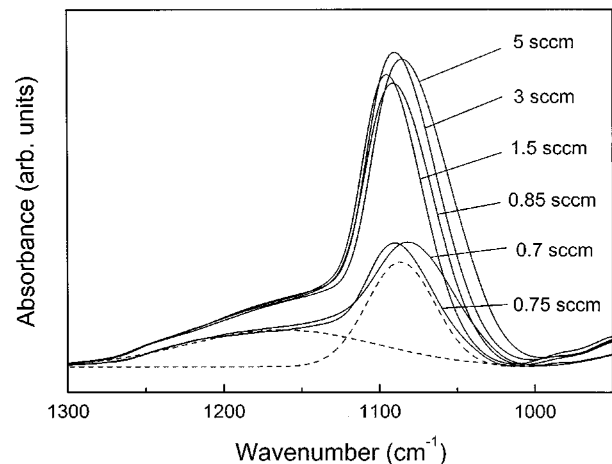

FIG. 6. FTIR spectra of SiOF films prepared at different H_2 flow rates in 950–1300 cm^{-1} region. The spectrum from the SiOF film prepared at 0.7 sccm of H_2 flow rate is deconvoluted to two Gaussian peaks located at about 1160 and 1090 cm^{-1} (shown by dashed lines) as an example.

modes of the Si–O–Si bonding, respectively. The Si–F_x absorption band is clearly seen in the 900-1000 cm^{-1} range. The ratio of the area of this band to the area of Si–O stretching vibration peak (Si–F/Si–O ratio) was used to estimate the fluorine content in our SiOF films. Figure 5 shows that the relationship between the F content and the H_2 flow rate is not a simple negative exponential, as it was expected on the basis of our previous studies.[17] On the contrary, an increase in the F content is observed as the H_2 flow rate increases in the range from 0.6 to 1.5 sccm. The exponential reduction in the F concentration is only observed at H_2 flow rates higher than 1.5 sccm. Si–H and Si–OH bond absorption peaks were absent in the FTIR spectra from as-deposited SiOF films in the entire range of H_2 flow rate.[17]

IR spectroscopy was employed for evaluating the structural characteristics of the films on the basis of works,[13,21–25] which relate the structural properties of silicon dioxide films with the form and characteristics of the IR absorption band associated with the Si–O–Si bond stretching vibrations in SiO_2 films. As can be observed in Fig. 6, the FWHM and position of this band shows significant changes as a function of H_2 flow rate. From these changes, the values of Si–O–Si angle deviation within SiOF network were calculated employing the equation used in Ref. 13. These values are shown in Fig. 7 and demonstrate that SiOF films deposited using H_2 flow rate below about 0.8 sccm are characterized by an increased angle deviation, which is indicative of their reduced structural homogeneity. It was also found that the ratio of the intensity of the high-wave number shoulder to the intensity of the main peak of the Si–O–Si stretching vibrations band undergo big changes as the H_2 flow rate changes. For the sake of the analysis, the band was deconvoluted using two Gaussian peaks. Figure 6 shows these contributions for a film deposited with a hydrogen flow rate of 0.75 sccm. In this case the main peak is located at 1090 cm^{-1} and the other one, which contributes to the high-wave number shoulder, is located at about 1160 cm^{-1}. The behavior of the intensity ratio between the high wave number peak and main peak as a function of H_2 flow rate is shown in Fig. 8. This ratio exhibits a trend consistent (opposite) with that of the refractive index (see Fig. 3) versus the H_2 flow rate. Namely, the

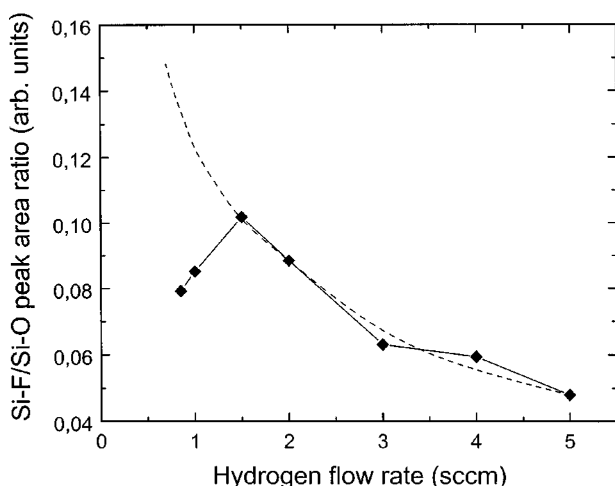

FIG. 5. Si–F/Si–O peak area ratio vs H_2 flow rate.

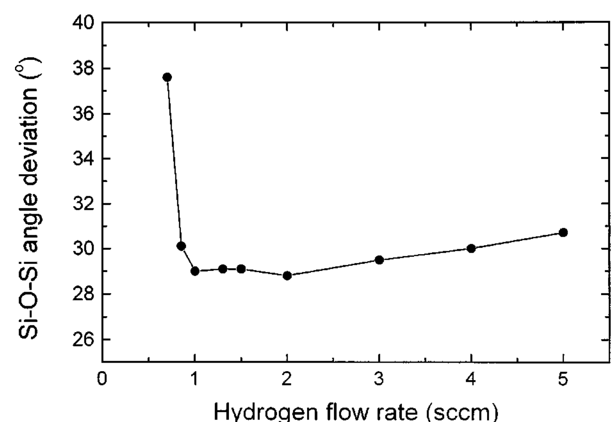

FIG. 7. Si–O–Si bond angle deviation as a function of H_2 flow rate.

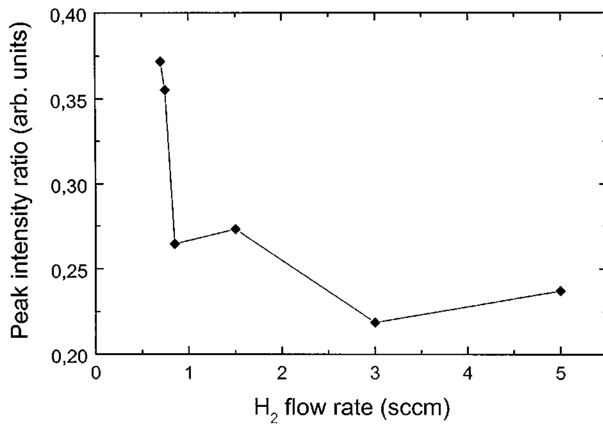

FIG. 8. Ratio in intensity of 1160 cm^{-1} Gaussian peak to that of the peak located at about 1090 cm^{-1} as a function of H_2 flow rate.

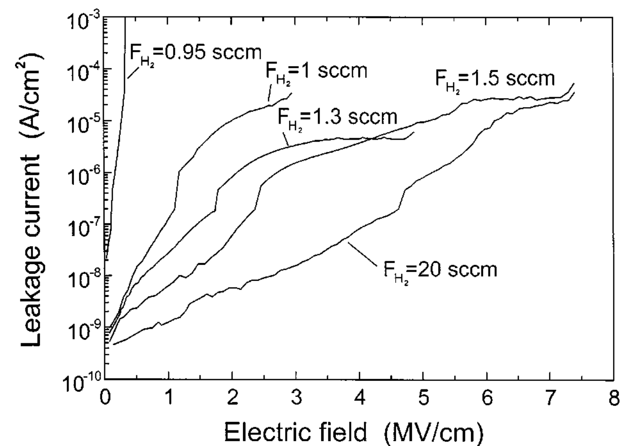

FIG. 10. Leakage current vs electric field of SiOF films prepared at different H_2 flow rates.

relative intensity of the high-wave number shoulder drastically increases when the H_2 flow rate reduces below 0.8 sccm.

Transmission electron microscopy (TEM) studies were performed for further investigation of the structure of SiOF films. Selected area electron diffraction studies showed that samples prepared at H_2 flow rates ranging from 0.6 to 10 sccm had a diffraction pattern [see inset in Figs. 9(a) and 9(b)], which consisted of a central halo and diffuse rings and indicated the structure of the films to be amorphous. This is consistent with a common concept of the SiO_2 film structure as a continuous random network of SiO_4 tetrahedra joined together by bridging oxygens.[20] Dark-field TEM did not show any presence of the crystalline phase in the samples prepared in the entire range of hydrogen dilution. However, bright-field TEM studies have revealed that the structure of the samples prepared at H_2 flow rates below about 0.8 sccm differed significantly from that of films prepared at higher hydrogen flow rates. As seen in Fig. 9(b), SiOF films prepared at H_2 flow rate exceeding 0.8 sccm are characterized by uniform homogenous structure typical for amorphous films. On the contrary, SiOF films prepared at the H_2 flow rate below about 0.8 sccm have the structure that can be classified as a biphase one as seen in Fig. 9(a). The microstructure of these films consists of the amorphous matrix, but with an incorporation of individual particles of the irregular shape and sized within 5–30 nm range.

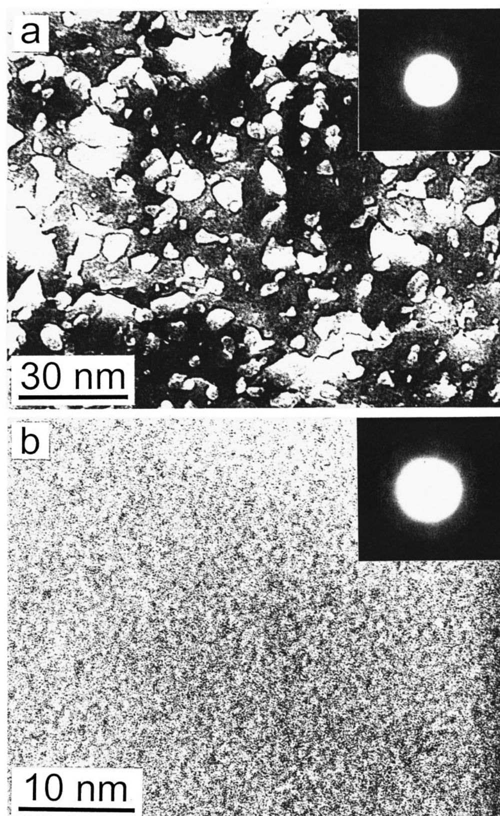

FIG. 9. (a) and (b) typical bright-field TEM images of the SiOF films prepared at the H_2 flow rate below and above 0.8 sccm, respectively, accompanied by corresponding selected area electron diffraction images (see insets).

B. Electrical properties

The electrical properties of the SiOF films as a function of H_2 flow rate were studied by taking I–V measurements on MOS capacitors which incorporated these films. The capacitor and equipment setup for these measurements was already described in Sec. II. Here it is only important to mention that the ramp rate was 0.5 V/s in the positive bias direction, i.e., a positive voltage was applied to the gate (aluminum electrode) in order to inject electrons from the n-type silicon substrate. Figure 10 shows the current–voltage characteristics obtained for SiOF films prepared at different H_2 flow rates. It is clearly seen that the leakage current of SiOF films increases as the H_2 flow rate decreases. Figure 11 shows the value of breakdown electric field of the samples as a function of H_2 flow rate. As seen in the figure, the SiOF films prepared at the H_2 flow rate above 1 sccm are stable at electric fields about 7 MV/cm. However, the dielectric integrity of films drops sharply when the H_2 flow rate decreases below about 1 sccm.

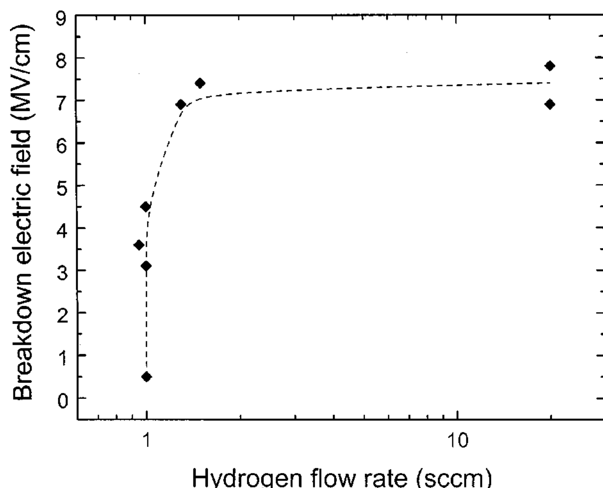

FIG. 11. Breakdown electric field as a function of H_2 flow rate.

IV. DISCUSSION

A. Deposition process and fluorine content

The behavior of the deposition rate shown in Fig. 1 can be explained considering that the SiOF film deposition process is indeed a continuous competition between two processes: (a) film growth by dissociation of SiF_4, followed by oxidation and reduction of SiF_x fragments with $x=1$, 2, 3, and (b) etching by highly reactive F species and hydrogen.[34–36] Based on this, it is clear that the deposition rate of the SiOF films should be very sensitive to the choice of operation conditions. In consistency with this, Han and Aydil[13] observed no SiOF film deposition if the SiF_4/O_2 flow rate ratio in SiF_4–O_2 gas mixture was above 1. No film growth took place either in the study of Kim *et al.*[14] when radio frequency power was below the threshold value of 1000 W. Our results evidently show that hydrogen dilution is able to effectively control the growth-etching equilibrium and even small hydrogen addition leads the process to shift from etching towards the film growth for a wide range of SiF_4/O_2 ratios (from 0.5 to 10), as seen in Fig. 2. The ability of hydrogen to control the etching-deposition transition has also been observed in SiF_4–H_2 systems for *a*-Si film growth[34] and can be attributed to both the ability of H to dissociate SiF_4 molecules giving free-bond silicon species ($-SiF_x$) and effective scavenging of free F radicals[2,4] yielding HF as a by-product of this reaction. HF is volatile and is removed from the reaction chamber by pumping. The saturation trend observed in Fig. 1 at high hydrogen flow rates likely corresponds to complete scavenging of F species by hydrogen. This is consistent with the finding that the film deposition rate saturates at higher H_2 flow rates with increasing flow rate of SiF_4. Indeed, the higher the SiF_4 flow rate, the higher concentration of reactive F species is produced, the higher hydrogen dilution is required to completely scavenge them.

The dependence of fluorine content in the films on the hydrogen flow rate shown in Fig. 5 can be explained on the same basis used in the previous paragraph. For example, the increase in the fluorine content as the H_2 flow rate increases in the range from 0.6 to 1.5 sccm can be due to the ability of H radicals to abstract halogen atoms from SiF_4.[34–36] Given this ability, at low hydrogen flow rates an increment in this flow rate can change the plasma chemistry in such a way that more SiF_x species are produced and incorporated in the film. Additionally, interaction of H_2 with electrons coming from the plasma region can cause changes in the electron energy distribution function similar to those observed in SiH_4–H_2 plasmas,[37] which can also enhance the production of SiF_x species to be incorporated into the films. It is also possible that the F content in as-deposited SiOF films prepared at H_2 flow rates below 1.5 sccm primary follows the exponential trend marked by the dashed curve in Fig. 5, but this trend considerably changes during postdeposition period due to intense F desorption. However, this question is out of the subject of the present work and requires additional studies. As mentioned in Sec. III, no bands related to hydrogen bonds were found in the IR spectra of our films. It must be pointed out that the IR absorption band observed in the range from 900 to 1000 cm^{-1} (see Fig. 4) was associated with Si–F bonds. This band cannot be due to Si–OH bonds since the IR absorption band associated with clustered OH(*s*) around 3350 cm^{-1} was not observed in any case. The absence of Si–OH or Si–H bonds in the films indicates that in spite of the fact that H_2 interacts with the SiF_4–O_2 mixture, the formation of Si–H and Si–OH bond during SiOF film growth is energetically less favorable than Si–F bonds probably due to the relatively high energy of the latter. On the other hand, atomic hydrogen is known to be very effective in releasing hydrogen weakly bound with silicon. For instance, Shimizu in his study observed that, despite introducing a large amount of atomic hydrogen during Si film deposition by glow discharge of SiF_4–H_2, the concentration of hydrogen in the film monotonously reduced down to 1–2 at. %.[36]

B. Film structure

1. Refractive index

It is known that the refractive index of any film is affected by its stoichiometry, type and amount of impurities, density, porosity, and stress. The determination of the influence of each one of these factors on the refractive index is a difficult task, especially in SiOF films because fluorine incorporation sensibly affects, at the same time, their density, porosity, stress and electronic polarizability of the oxide. However, based on our results, in the following sections we have made an attempt to evaluate separately the contribution of some of these factors on the refractive index of our films. Since Rutherford backscattering spectroscopy (RBS) measurements have shown that all our samples were nearly stoichiometric (Si:O=1:2) we have only discussed the contribution of factors other than stoichiometry.

2. Contribution of electronic polarizability

One important contribution to decrease the refractive index of SiOF films is the reduction in their electronic polarizability due to the amount of F atoms incorporated into the SiO_2 network.[16] The trend generally found is that the refrac-

tive index decreases as the fluorine content increases. It is worth noting that reported values of the refractive index for high-fluorinated SiOF films are typically in the 1.38–1.43 range, for fluorine concentration in the films as high as 15 at.%.[3,9–11] Figures 3 and 5 show that our SiOF films prepared at H_2 flow rates higher than 1.5 sccm follow the general trend. However, SiOF films deposited at H_2 flow rates below 1.5 show the opposite trend. In fact, the SiOF film deposited at a flow rate of 0.8 sccm is characterized by an extremely small refractive index of 1.2 and the smallest amount of fluorine incorporated. On the contrary, the film deposited at 1.5 sccm has a higher fluorine content, however it has a refractive index exceeding the value of 1.4. It allows us to exclude the reduction in the electronic polarizability as the main factor contributing to the low values of refractive index observed in films deposited in the 0.6–1.5 sccm range of H_2 flow rate. It also suggests that other factors are responsible for the observed changes in the refractive index, namely decrease in the film density and intrinsic stress.

3. Contribution of continuous changes in film density

Various mechanisms can contribute to the reduction in the SiOF film density. One of them is the presence of voids in the form of connected or isolated pores. Another one is the formation of a highly open SiOF network built from high-order Si–O–Si ring units.[38] The internal space of such rings can be considered as individual nanovoids. As was shown in our previous studies[17,38] the average order of ring units within the SiOF network should increase with the fluorine content resulting in a continuous SiOF film density reduction. As mentioned previously, Figs. 3 and 5 demonstrate that SiOF films with a refractive index of 1.2 have a moderate fluorine content. Consequently, these films must contain a small amount of nanovoids, whereas those characterized by a refractive index of about 1.4 must contain more fluorine and consequently more nanovoids. This suggests that the low refractive index of SiOF films deposited in the 0.6–1 sccm H_2 flow rate range is not due to the continuous reduction in the density of the films produced by the presence of nanovoids but rather due to isolated pores (porosity) in the films.

4. Contribution of film porosity

As shown in Sec. III, the form of the IR stretching mode of the Si–O–Si bonding changes as hydrogen dilution changes. Specifically, Fig. 8 shows that the intensity of the high-wave number shoulder of the stretching band increases sharply with respect to the intensity of the main peak as hydrogen flow rate decreases below 1 sccm. As discussed below, these changes can be correlated with porosity and/or other structural changes in the films. The shoulder of the stretching band located at about 1200 cm^{-1} is attributed to the out-of-phase motion of adjacent oxygen atoms of the asymmetric stretching transverse optical (AS_2TO) vibration, whereas the main absorption band at about 1090 cm^{-1} is assigned to the AS_1TO in-phase motion of adjacent oxygens.[23,24] Kirk has shown in a quantitative study of the IR absorption spectra of thermally grown SiO_2 films that the AS_2TO mode mainly contributing to the high-frequency shoulder is due to a disorderinduced mechanical coupling between the AS_1 and AS_2 modes.[26] Therefore, any factor causing structural nonuniformity in the surrounding vibrational units (including the deviation from stoichiometry, the presence of nonbridging oxygen atoms, impurities, porosity, stress, etc.) can cause perturbation and resultant modifications in the AS_2TO mode.[23–33] Some systematic studies relating the height of the shoulder of the Si–O–Si stretching vibration mode with film composition have found that modifications in the stoichiometry of the SiO_2 films toward the silicon rich composition increase the height of this shoulder with respect to the height of the main peak.[24,25] On the other hand, several recent works have suggested that the high-wave number shoulder of the Si–O–Si stretching vibration mode is related to the porosity of the material in such a way that the ratio of intensity between this shoulder and the main peak increases as film porosity increases.[29–33] It is worth mentioning that these studies were carried out on SiO_2 films prone to be porous, since most of them were deposited at very low temperatures by techniques such as spin coating of silica sol gel (room temperature),[29] photo-CVD (80 °C),[30] PECVD (30 °C),[31] liquid phase deposition (50 °C),[32] and electron-beam evaporation (20 °C).[33] Additionally, the density and refractive index of some of these films was as low as 1.49 g/cm^3 and 1.1, respectively.[31,32] Based on these works and taking into account that, according to RBS measurements, our films are nearly stoichiometric, we can suppose that the considerable reduction in the refractive index and the drastic increase in the relative intensity of the high-frequency shoulder (see Figs. 3 and 8) of our SiOF films prepared at H_2 flow rates below 0.8 sccm are due to porosity in the films. However, as is discussed below using TEM results, the porosity in these films can be typified as formed by closed voids.

The contribution of intrinsic stress is not clear at present, however it can probably be neglected since a fixed oxide structure distorted by the stress normally exhibits more significant changes in the infrared absorption strength of the shoulder relative to the main peak of the Si–O–Si stretching band. For example, it has been reported that an oxide film under stress undergoes structural rearrangement to relieve the stress and might reveal a strong absorption band between 1150 and 1250 cm^{-1} and the virtual disappearance of the 1080 cm^{-1} peak.[39] As seen in Figs. 6 and 8, the Si–O–Si stretching vibrational mode of our SiOF films does not show any of the aforementioned extreme changes in the entire range of H_2 flow rates.

C. Nature and origin of film porosity

TEM results revealed that our SiOF films deposited at hydrogen flow rates below 0.8 sccm have a biphase structure, which consists of individual particles of irregular shape and size (5–30 nm) embedded in an amorphous matrix. Since both dark-field TEM and selected area electron diffraction did not reveal any presence of polycrystalline phase, we can suppose that these particles also have an amorphous struc-

ture. IR results are consistent with the TEM results since the values of Si–O–Si angle deviation within SiOF network, shown in Fig. 7, demonstrate that SiOF films with biphase microstructure (H_2 flow rate below about 0.8 sccm) are characterized by an increased angle deviation, which is indicative of their reduced structural homogeneity.

The most probable explanation of the biphase microstructure formation in films deposited at very low hydrogen flow rates is a gas phase oxidation of SiF_x fragments (with $x=1$, 2, 3) in plasma and downstream region followed by their incorporation into the growing amorphous SiOF film. Since the image of these particles in the micrograph is much lighter than that of the matrix [see Fig. 9(a)], it allows us to suppose that the density of these particles is less than that of surrounding SiOF network. As a consequence, SiOF films with biphase structure must have a reduced density. Since the orientation of the incoming flux during remote PECVD is well defined, the presence of irregularly shaped foreign particles on the film surface can act as local masks producing the effect of shadowing. The surface mobility of precursors during low-temperature remote PECVD is not sufficient to provide a conformous coating growth. In these conditions it is very probable the formation of closed voids (porous) in the area of shadow which additionally contributes to the reduction in the density of SiOF films. In summary, the structure of these films can be typified as a biphase-porous structure formed by a SiOF network with amorphous low density particles and closed voids embedded on it.

When the H_2 flow rate exceeds 0.8 sccm the particles are not observed in the film [see Fig. 9(b)]. This allows us to assume that the presence of hydrogen in the reaction chamber at a certain concentration is able to effectively suppress the gas phase oxidation of SiF_x species preventing thereby the particle incorporation into the growing amorphous SiOF network. The mechanism of hydrogen action is not clear at the moment, however it is known for SiF_4–H_2 plasmas that an interaction of SiF_x fragments ($x=1$, 2, or 3) with atomic hydrogen in gas phase can lead to the production of various SiF_nH_m neutral and ionized species (m, $n=1$, 2, or 3, $n+m<3$).[34–36] It has been found that Si–F bonds formed in *a*-Si:H(F) films prepared by glow discharge of SiF_4–H_2 are easily changed into Si–O–Si ones as a result of Si–F bond hydrolysis when the films are exposed to the air.[36] Thus, in the presence of oxygen, hydrogen and fluorine radicals in SiF_4–O_2–H_2–He plasmas a continuous competition should exist in the passivation of SiF_x species dangling bonds by O, H, or F. It is obvious that the probability of Si dangling bond termination by hydrogen is increased with H_2 flow rate. At present it is not clear whether SiF_nH_m or $SiO_xF_nH_m$ species are the resulting by-products of the above processes. However, the finding that no particle incorporation takes place when the H_2 flow rate exceeds about 0.8 sccm allows us to suppose that the presence of H radicals in the reaction chamber effectively suppresses gas phase oxidation of SiF_x precursors favoring thereby the formation of homogeneous high-dense amorphous SiOF films.

D. Electrical properties

I–V measurement results (Figs. 10 and 11) show that there is a strong correlation between the electrical properties and the structural changes observed in SiOF films as a function of H_2 flow rate. Films deposited at hydrogen flow rates higher than 1 sccm are structurally and electrically superior than films deposited at lower flow rates. The dielectric integrity is practically lost and there is a drastic structural degradation when the SiOF films are deposited at H_2 flow rate below about 1 sccm. From this correlation we can conclude that the structural defects in these biphase and porous SiOF films create a great amount of electronic defects and cause the total deterioration of their insulating properties.

V. CONCLUSIONS

Analysis of the experimental data has demonstrated that the structural and electrical properties of SiOF films prepared from SiF_4–O_2–He–H_2 based plasmas depend sensibly on hydrogen flow rate and change drastically at low hydrogen dilution. The correlation among these changes and the changes in deposition rate indicate that hydrogen added into the SiF_4/O_2/He plasma is effective not only to scavenge F species but also to control the amount of gas phase reactions and provoke the etching-deposition transition for SiOF film growth. When the addition of hydrogen into the SiF_4–O_2–He feedstock gas mixture is less than 0.8 sccm, the SiOF films obtained have extremely low deposition rate and are characterized by biphase microstructure consisting of an amorphous matrix with an incorporation of individual particles of the irregular shape and sized within 5–30 nm range. The origin of the above particles is assumed to be gas phase oxidation of SiF_x species (with $x=1$, 2, 3) in plasma and downstream regions. It has been shown that building up the above particles into the growing amorphous SiOF network results in the formation of a low density inhomogeneous and porous structure and leads to considerable degradation of electrical properties of SiOF films. It has also been revealed that addition of hydrogen to the feedstock gas mixture in quantities higher than 0.8 sccm effectively suppresses the particles incorporation into the SiOF matrix probably through hindering of gas phase oxidation of SiF_x species. SiOF films prepared in these conditions are characterized by homogeneous high-dense amorphous microstructure and good electrical properties (leakage current is less than 4×10^{-4} A/cm^2 at the breakdown electric field of at least 7 MV/cm).

Lowering the value of the refractive index of SiOF films below 1.3 is assumed to be an indicator of their reduced density rather than a reduction in electronic polarizability in the entire range of F doping level.

ACKNOWLEDGMENTS

The authors want to acknowledge S. Jiménez for her technical assistance. This work was partially supported by CONACyT under Project No. 26423-A, and by DGAPA under Project No. IN100997.

[1]J. Song, P. K. Ajmera, and G. S. Lee, Appl. Phys. Lett. **69**, 1876 (1996).
[2]T. Tamura, J. Sakai, M. Satoh, Y. Inoue, and H. Yoshitaka, Jpn. J. Appl. Phys., Part 1 **36**, 1627 (1997).
[3]W. S. Yoo, R. Swope, and D. Mordo, Jpn. J. Appl. Phys., Part 1 **36**, 267 (1997).
[4]L. Q. Qian, H. W. Fry, G. Nobinger, J. T. Pye, M. C. Schmidth, J. Cassillas, and M. Lieberman, *Proceedings of the First International VMIC Specialty Conference on Dielectrics for ULSI Multilevel Interconnection* (DUMIC, 1995), p. 50.
[5]K. M. Chang, S. W. Wang, T.H. Yeh, C. H. Li, and J. J. Luo, J. Electrochem. Soc. **144**, 1754 (1997).
[6]H. Kudo, R. Shinohara, S. Takeishi, N. Awaji, and M. Yamada, Jpn. J. Appl. Phys., Part 1 **35**, 1583 (1996).
[7]M. Yoshimaru, S. Koizumi, and K. Shimokawa, J. Vac. Sci. Technol. A **15**, 2915 (1997).
[8]M. K. Bhan, J. Huang, and D. Cheung, Thin Solid Films **308–309**, 507 (1997).
[9]M. T. Weise, S. C. Selbrede, L. J. Arias, and D. Carl, J. Vac. Sci. Technol. A **15**, 1399 (1997).
[10]V. L. Shannon and M. Z. Karim, Thin Solid Films **270**, 498 (1995).
[11]T. Usami, K. Shimokawa, and M. Yoshimaru, Jpn. J. Appl. Phys., Part 1 **33**, 408 (1994).
[12]S. W. Lim, Y. Shimogaki, Y. Nakano, K. Tada, and H. Komiyama, Jpn. J. Appl. Phys., Part 1 **35**, 1468 (1996).
[13]S. M. Han and E. S. Aydil, J. Vac. Sci. Technol. A **15**, 2893 (1997).
[14]J.-H. Kim, S.-H. Seo, S.-M. Yun, H.-Y. Chang, K.-M. Lee, and C.-K. Choi, Appl. Phys. Lett. **68**, 1507 (1996).
[15]S. Lee and J.-W. Park, Mater. Chem. Phys. **53**, 150 (1998).
[16]S. M. Han and E. S. Aydil, J. Appl. Phys. **83**, 2172 (1998).
[17]V. Pankov, J. C. Alonso, and A. Ortiz, Jpn. J. Appl. Phys., Part 1 **37**, 6135 (1998).
[18]A. Matsuda, J. Non-Cryst. Solids **59–60**, 757 (1983).
[19]C. Falcony, J. C. Alonso, A. Ortiz, M. Garcia, E. P. Zironi, and J. Rickards, J. Vac. Sci. Technol. A **11**, 2945 (1993).
[20]P. N. Sen and M. F. Thorpe, Phys. Rev. B **15**, 4030 (1977).
[21]J. T. Fitch, E. Kobeda, G. Lucovsky, and E. A. Irene, J. Vac. Sci. Technol. B **7**, 153 (1989).
[22]J. T. Fitch, S. S. Kim, and G. Lucovsky, J. Vac. Sci. Technol. A **8**, 1871 (1990).
[23]G. Lucovsky, C. K. Wong, and W. B. Pollard, J. Non-Cryst. Solids **59–60**, 839 (1983).
[24]P. G. Pai, S. S. Chao, Y. Takagi, and G. Lucovsky, J. Vac. Sci. Technol. A **4**, 689 (1986).
[25]E. Fogarassy, A. Slaoui, C. Fuchs, and J. L. Regoline, Appl. Phys. Lett. **51**, 337 (1987).
[26]C. T. Kirk, Phys. Rev. B **38**, 1255 (1988).
[27]P. Lange, J. Appl. Phys. **66**, 201 (1989).
[28]W. Bensch and W. Bergholz, Semicond. Sci. Technol. **5**, 421 (1990).
[29]R. M. Almeida and C. G. Pantano, J. Appl. Phys. **68**, 4225 (1990).
[30]R. Ashokan, R. Singh, V. Gopal, and M. Anandan, J. Appl. Phys. **73**, 3943 (1993).
[31]A. Goullet, C. Charles, P. García, and G. Turban, J. Appl. Phys. **74**, 6876 (1993).
[32]J.-S. Chou and S.-C. Lee, J. Appl. Phys. **77**, 1805 (1995).
[33]A. Brunet-Bruneau, J. Rivory, B. Rafin, J. Y. Robic, and P. Chaton, J. Appl. Phys. **82**, 1330 (1997).
[34]G. Bruno, P. Capezzuto, and G. Cicala, J. Appl. Phys. **69**, 7256 (1991).
[35]S. Oda, S. Ishihara, N. Shibata, H. Shirai, A. Miyauchi, K. Fukuda, A. Tanabe, H. Ohtoshi, J. Hanna, and I. Shimizu, Jpn. J. Appl. Phys., Part 2 **25**, L188 (1986).
[36]I. Shimizu, J. Non-Cryst. Solids **97–98**, 257 (1987).
[37]M. Capitelli, C. Gorse, R. Winkler, and J. Wilhelm, Plasma Chem. Plasma Process. **8**, 399 (1988).
[38]V. Pankov, J. C. Alonso, and A. Ortiz, J. Appl. Phys. **86**, 275 (1999).
[39]J. E. Olsen and F. Shimura, Appl. Phys. Lett. **53**, 1934 (1988).